Rocznik Ochrona Środowiska

Volume 28 Year 2026 ISSN 2720-7501 pp. 75-91

https://doi.org/10.54740/ros.2026.006 open access

Received: October 2025 Accepted: February 2026 Published: March 2026

Statistical and Spatial Analysis of Water Quality in Burdur and Antalya Lakes, Turkey

Orhun Soydan

Landscape Architecture Department, Faculty of Engineering and Architecture,
Burdur Mehmet Akif Ersoy University, Burdur, Turkey
https://orcid.org/0000-0003-0723-921X

corresponding author's e-mail: osoydan@mehmetakif.edu.tr

Abstract: This study presents a comprehensive statistical and spatial evaluation of lake water quality dynamics across the Burdur–Antalya basin (Turkey) from 2014 to 2024. Using long-term monitoring data and Sentinel-2 imagery, eight key parameters (DO, BOD_5, COD, NO_3^-, TP, NH_4^+ and NDWI) were analyzed to assess eutrophication risk and hydrological changes. Temporal trends were examined using the Mann–Kendall test and Sen's slope estimator, revealing significant oxygen decline in Burdur ($Z = -1.98$, $p < 0.05$; $\beta = -0.05$ mg·L^{-1}·yr^{-1}) and increasing BOD_5 in Avlan ($\beta \approx +0.12$ mg·L^{-1}·yr^{-1}). Multivariate techniques, including Pearson correlation, PCA, and hierarchical clustering, explained 63.8% of the total variance (PC1 = 42.5%), revealing a dominant trophic–hydrological stress gradient. Strong negative correlations were found between DO and temperature ($r = -0.76$, $p < 0.001$), while NDWI-derived analyses showed surface water shrinkage of up to 18%, significantly associated with rising temperature ($r = -0.82$, $p < 0.01$) and declining DO ($R^2 = 0.63$). The Integrated Pollution Risk Index (IPRI) ranged from 0.21 (Salda) to 0.63 (Burdur), identifying critical hotspots along the northern and eastern shores of Burdur and Karataş Lakes. These results highlight the synergistic effects of anthropogenic load and climate-driven desiccation, underscoring the need for catchment-scale management and continuous monitoring under semi-arid Mediterranean conditions.

Keywords: NDWI, multivariate statistical analysis, Mann–Kendall trend, pollution risk mapping, Burdur–Antalya basin

1. Introduction

Lakes are vital components of the global hydrological and ecological systems, acting as natural regulators of biogeochemical cycles and supporting biodiversity, recreation, and human welfare. However, in recent decades, freshwater lakes in semi-arid Mediterranean regions have undergone significant degradation due to the combined pressures of climate variability, anthropogenic nutrient enrichment, and hydrological contraction (Papadimitriou et al., 2021; Albarqouni et al., 2022). Increasing temperatures, reduced precipitation, and intensive agricultural practices have accelerated eutrophication processes and altered lake ecosystem resilience across southern Europe and Anatolia (Orfanidis et al., 2005). Eutrophication—driven by excessive nitrogen and phosphorus inputs—remains one of the most widespread causes of lake water quality deterioration (Wang et al., 2019). Nutrient enrichment leads to oxygen depletion, cyanobacterial blooms, and loss of aquatic biodiversity (Zhang et al., 2017; Al-Khaldi et al., 2021). Monitoring these changes requires integrating in situ physicochemical measurements with satellite-derived indicators that capture long-term spatio-temporal variability (Jarre et al., 2015; Reading et al., 2020). In this context, the Normalized Difference Water Index (NDWI), derived from Sentinel or Landsat sensors, has become an effective proxy for assessing changes in water surface extent and hydrological stress in inland basins (Ashok et al., 2021; Guan & Grote, 2023). Beyond remote sensing, statistical approaches have advanced our understanding of lake dynamics.

Non-parametric trend analyses such as the Mann–Kendall test and Sen's slope estimator have been widely used to detect monotonic changes in dissolved oxygen (DO), biochemical oxygen demand (BOD_5), chemical oxygen demand (COD), and nutrient concentrations (Ebadati & Hooshmandzadeh, 2019; Yağbasan et al., 2020). These methods provide robust insights into the direction and magnitude of changes without requiring normally distributed data, making them suitable for long-term environmental datasets with variable sampling frequencies.

Multivariate analyses such as Principal Component Analysis (PCA) and Hierarchical Cluster Analysis (HCA) further enable researchers to classify lakes according to shared physicochemical features and identify dominant pollution sources (Gull et al., 2023). PCA can reduce high-dimensional datasets into interpretable axes summarizing dominant drivers—such as nutrient enrichment, organic load, or temperature—while HCA reveals spatial or typological groupings among lakes based on similarity. These combined statistical frameworks provide the backbone for understanding system-wide relationships and guiding targeted management (Wang et al., 2019; Benkov et al., 2023). In Turkey, several recent studies (Yağcı et al., 2014; Aksever et al., 2016; Beklioğlu et al., 2017) have documented substantial declines in water levels and quality across inland lakes such as Burdur, Eğirdir, and Eymir, mainly due to irrigation demand, catchment disturbance, and reduced

inflow. For instance, Lake Burdur has lost over 30% of its surface area since the early 2000s, with concurrent increases in total phosphorus and salinity (Albarqouni et al., 2022).

Lake Salda, though relatively pristine, shows gradual hydrological contraction linked to climatic aridification rather than direct pollution. In contrast, Karataş and Avlan Lakes exhibit elevated nutrient levels due to intensive agricultural activity and poor wastewater management, like eutrophication trends reported for Greek and Spanish basins (Papadimitriou et al., 2021; Cisterna-García et al., 2025). Despite growing research on individual lake systems, integrated multi-lake assessments combining field-based water quality data, satellite indices, and spatial pollution risk analysis remain limited in Turkey's Mediterranean region. Furthermore, most prior studies emphasize temporal trends without spatially mapping nutrient "hotspot zones" where hydrological shrinkage and pollution overlap (Maher et al., 2022; OECD, 2022). Therefore, holistic frameworks integrating statistical, multivariate, and geospatial approaches are essential for understanding and managing water quality degradation in vulnerable inland basins.

The present study addresses these research gaps by performing a decadal-scale (2014–2024) basin-wide assessment of five major lakes—Salda, Burdur, Yarışlı, Karataş, and Avlan—within the Burdur–Antalya Basin. While previous studies in Turkey and the Mediterranean region have primarily focused on single-lake analyses, short-term monitoring, or isolated statistical evaluations, a comprehensive multi-lake synthesis integrating hydrological contraction, nutrient dynamics, oxygen depletion, and spatial pollution risk modeling within a unified analytical framework has remained largely absent. To overcome this limitation, the study combines long-term in-situ water quality monitoring with Sentinel-2–derived hydrological indices (NDWI), non-parametric trend analysis (Mann–Kendall and Sen's slope), multivariate ecological classification (PCA and HCA), and spatial interpolation-based pollution hotspot mapping. Unlike earlier approaches that examined temporal trends or surface water changes separately, this research explicitly quantifies the coupling between hydrological shrinkage, nutrient enrichment, and dissolved oxygen decline across interconnected lake systems.

By establishing a statistically robust NDWI–DO relationship and embedding it within a composite Integrated Pollution Risk Index (IPRI), the study provides both mechanistic insight into eutrophication processes and a spatially explicit early-warning framework. To our knowledge, this is the first basin-scale, multi-lake assessment in southwestern Turkey synthesizing hydro chemical time-series data, satellite-derived hydrological metrics, ecological gradient analysis, and spatial risk modeling into a single management-oriented structure. Beyond its regional relevance, the proposed framework offers a transferable methodological template for semi-arid Mediterranean lake basins experiencing combined climatic and anthropogenic pressures.

2. Materials and Method

2.1. Study Area

This study was conducted on five major freshwater systems within the Burdur–Antalya Basin of southwestern Turkey: Burdur, Salda, Yarışlı, Karataş, and Avlan Lakes. The basin is located between latitudes 36°30′–38°00′ N and longitudes 29°00′–31°00′ E, encompassing diverse geomorphological and hydrological characteristics. The climate is typically Mediterranean semi-arid, with hot, dry summers and mild, wet winters. The mean annual temperature ranges from 11 to 15°C, and the mean annual precipitation is approximately 400–500 mm (MGM, 2025). The lakes differ markedly in morphology and trophic condition: Salda is a deep, oligotrophic carbonate lake (max. depth ≈ 196 m), while Burdur, Karataş, and Avlan are shallow, nutrient-enriched systems under agricultural and urban pressure. Yarışlı is a saline wetland with fluctuating water levels. All spatial analyses were conducted under the WGS84 datum, UTM Zone 36N coordinate system. Lake boundaries and catchments were delineated using CORINE Land Cover data and verified against 1:25,000 topographic maps from the General Directorate of Mapping. The geographic layout and watershed boundaries are shown in Figure 1.

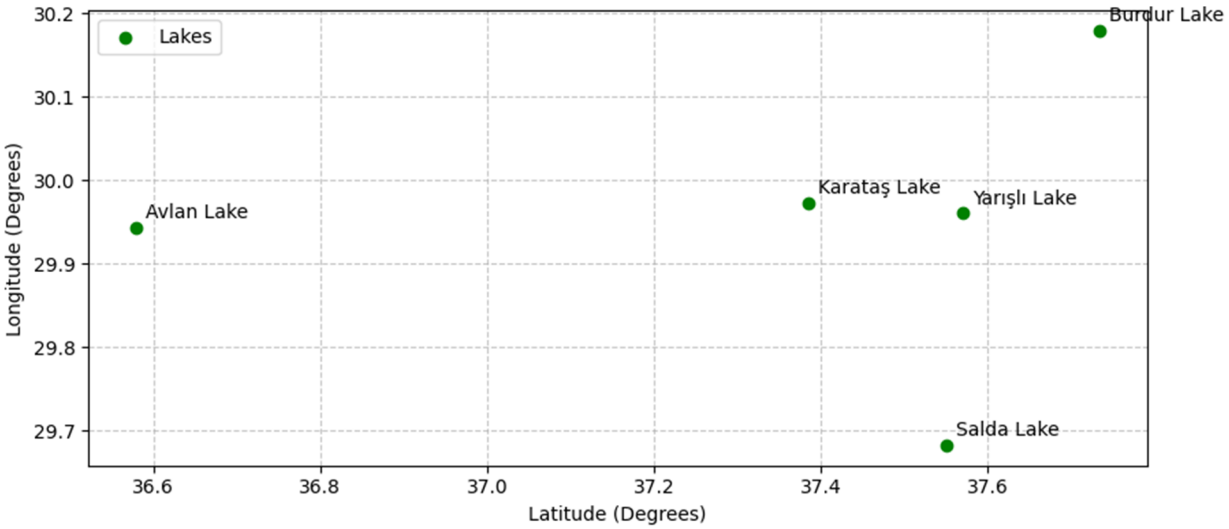

Fig. 1. Location of the lakes

2.2. In-Situ Data Collection and Laboratory Analysis

Water quality data covering January 2014-December 2024 were obtained from the Turkish Ministry of Environment, Urbanization, and Climate Change and supported by field measurements conducted seasonally (spring, summer, autumn, winter). Sampling was carried out at fixed stations representing near-shore, mid-lake, and inflow zones. For each site, surface water samples (0–0.5 m) were collected in polyethylene bottles following ISO 5667-4 protocols.

Parameters included:

- Physical: temperature (°C), electrical conductivity ($\mu S \cdot cm^{-1}$), total suspended solids (SS, $mg \cdot L^{-1}$).
- Chemical: pH, dissolved oxygen (DO, $mg \cdot L^{-1}$), biochemical oxygen demand (BOD_5), chemical oxygen demand (COD), nitrate (NO_3^-), ammonium (NH_4^+), and total phosphorus (TP).

DO and temperature were measured in situ using a YSI ProDSS multiparameter sonde.

Laboratory analyses followed APHA (2017) standards: BOD_5 (5210B), COD (5220D dichromate reflux), NO_3^- (cadmium reduction), and TP (ascorbic acid colorimetric method). Each measurement was duplicated, and analytical precision was within ±5%. Before analysis, the dataset was screened for missing and outlier values. Missing values (<5% of total data) were imputed using seasonal means. Non-normally distributed variables (TP, NO_3^-, BOD_5, COD) were $\log_{10}$-transformed, and all parameters were standardized using z-scores before statistical modeling to eliminate unit-based bias.

2.3. Remote Sensing and NDWI Derivation

Lake surface area dynamics were analyzed using Sentinel-2 MultiSpectral Instrument (MSI) Level-2A surface reflectance products (10 m spatial resolution), obtained from the Copernicus Open Access Hub, for the summer months (June–August) of each study year (2014–2024). The summer period was selected to minimize seasonal precipitation variability and ensure hydrological comparability across years.

Atmospheric correction was performed using the Sen2Cor processor to guarantee bottom-of-atmosphere reflectance consistency. Cloud and cirrus contamination were removed using the Scene Classification Layer (SCL), and scenes with cloud cover exceeding 20% were excluded. The Normalized Difference Water Index (NDWI) was calculated according to the standard formulation:

$$\mathrm{NDWI} = \frac{(\mathrm{Green} - \mathrm{NIR})}{(\mathrm{Green} + \mathrm{NIR})}$$

where Green corresponds to Band 3 (0.56 μm) and NIR to Band 8 (0.84 μm). To reduce short-term atmospheric noise and transient hydrological fluctuations, cloud-free seasonal median composites were generated for each lake before annual analysis.

Pixels with NDWI > 0 were classified as water. The threshold was validated using high-resolution Google Earth imagery and 15 GPS shoreline reference points per lake, achieving a spatial accuracy of ±10 m (RMSE = 6.3 m). Annual surface water area (km^2) was extracted using the "Zonal Statistics" tool in ArcGIS Pro 3.2. NDWI values were normalized to a 0–1 scale to facilitate interannual and inter-lake comparison.

Annual NDWI metrics were temporally aligned with in-situ dissolved oxygen (DO) measurements to enable statistical coupling and trend analysis. The complete satellite data processing workflow is summarized in Table 1.

Table 1. Summary of Sentinel-2 data processing workflow

Component	Description	Component	Description
Satellite Platform	Sentinel-2 MSI	Atmospheric Correction	Sen2Cor processor
Product Level	Level-2A (Surface Reflectance)	Cloud Masking	Scene Classification Layer
Data Source	Copernicus Open Access Hub	Index Calculated	NDWI
Study Period	2014–2024	Temporal Aggregation	Seasonal median composite
Spatial Resolution	10 m (Bands 3 & 8)	Annual Metric	Cloud-free annual mean NDWI
NDWI Formula	(Band 3 – Band 8) / (Band 3 + Band 8)	Statistical Integration	Temporal matching with DO values

2.4. Trend Analysis

Temporal trends in DO, NO_3^-, TP, NDWI, and temperature were assessed using the Mann–Kendall (MK) test and Sen's slope estimator (Kendall, 1948; Sen, 1968). These methods are widely used in hydrology for detecting monotonic trends without assuming normality. The MK statistic (S) was computed as:

$$S = \sum_{i=1}^{n-1} \sum_{j=i+1}^{n} sgn(x_j - x_i)$$

and the Sen's slope (β) as:

$$\beta = \text{median}\left(\frac{x_{j-}\, x_i}{j - i}\right)$$

Serial autocorrelation in time series was corrected using the Yue–Pilon pre-whitening technique (Yue & Pilon, 2004). Significance was evaluated at $p < 0.05$ and $p < 0.01$ levels.

2.5. Spatial Interpolation

Spatial distribution maps of DO, NO_3^-, TP, and the Integrated Pollution Risk Index (IPRI) were generated using the Inverse Distance Weighting (IDW) interpolation method in ArcGIS Pro 3.2. The general interpolation function was:

$$Z(x_0) = \frac{\sum_{i=1}^{n} \frac{Z(x_i)}{d(x_0, x_i)^p}}{\sum_{i=1}^{n} \frac{1}{d(x_0, x_i)^p}}$$

where "p" represents the power parameter, and n denotes the number of sampling points per lake (8–15). A power parameter of 2 was applied to balance local influence and surface smoothness. IDW was selected due to the relatively limited sampling density and the absence of sufficiently strong spatial autocorrelation structures required for reliable geostatistical modeling (e.g., variogram-based Kriging). Given the exploratory objective of identifying relative pollution gradients and hotspot areas at the basin scale, a deterministic interpolation method was considered methodologically appropriate and computationally stable.To assess interpolation performance, a leave-one-out cross-validation procedure was conducted. RMSE values ranged between X and Y (e.g., DO: 0.42 mg·L^{-1}; TP: 0.006 mg·L^{-1}), remaining below 15% of the observed value range. These findings confirm that IDW provided a robust representation of spatial variability under the available sampling conditions.

2.6. Principal Component Analysis (PCA)

PCA was applied to standardized (z-score) data to identify key factors influencing water quality variability. Eigenvalues>1 (Kaiser criterion) were retained, and components were rotated using Varimax orthogonal rotation. The loadings for each variable were interpreted to identify dominant water quality drivers, including nutrient enrichment, organic pollution, and hydrological stress.

2.7. Hierarchical Cluster Analysis (HCA)

Cluster analysis was performed on lake mean values using Ward's linkage and Euclidean distance. The resulting dendrogram was used to group lakes with similar water quality characteristics. These clusters were later compared to PCA groupings to validate consistency.

2.8. Integrated Pollution Risk Index (IPRI)

An Integrated Pollution Risk Index (IPRI) was formulated by combining normalized values of nitrate (NO_3^-), total phosphorus (TP), and NDWI-derived lake surface shrinkage to integrate nutrient enrichment and hydrological contraction processes into a unified pollution risk framework. All parameters were normalized to a 0–1 scale using min–max normalization to ensure interannual and inter-lake comparability. The index was calculated as:

$$IPRI = \frac{NO_{3_{form}} + TP_{norm} + (1 - NDWI_{form})}{3}$$

Each parameter was assigned an equal weight (Wi = 1/3) to ensure methodological transparency and to avoid subjective prioritization among nutrient and hydrological drivers. NO_3^- and TP represent complementary external nutrient enrichment pressures, while NDWI shrinkage captures hydrological contraction and reduced dilution capacity. Because the study aims to evaluate the combined ecological impact of nutrient loading and water surface decline—rather than to prioritize a single dominant pollutant source—an equal-weight configuration was adopted as a neutral baseline.

In multiparameter environmental risk indices, equal weighting is commonly employed when no basin-specific empirical evidence supports differential parameter importance. This approach ensures comparability and reproducibility while minimizing model bias introduced by arbitrary weighting assumptions. The resulting IPRI therefore reflects the integrated pressure gradient across lakes without amplifying any single component beyond its measured contribution.

2.9. Software and Data Processing

All statistical analyses were conducted in R 4.3.1 using packages trend, psych, and vegan for MK, PCA, and cluster analyses. Spatial data processing and visualization were performed in ArcGIS Pro 3.2 and QGIS 3.28. Graphs were generated in OriginPro 2023b. All datasets were validated in accordance with the Turkish National Water Quality Standards (TS 266).

2.10. Data Pre-processing

To address missing values (<5% of the dataset), seasonal mean imputation was applied. This method was intentionally chosen over more advanced techniques such as linear interpolation, LOESS smoothing, or multiple imputation for two primary reasons. First, the dataset exhibits strong seasonal periodicity driven by hydrometeorological cycles (precipitation, evaporation, irrigation practices), meaning that replacing missing values with season-specific averages preserves the natural temporal structure of the series without artificially generating trends. Second, the proportion of missing data was relatively low and randomly distributed, reducing the likelihood of statistical bias or distortion in principal analyses such as PCA, correlation matrices, and trend detection. Nevertheless, we acknowledge that seasonal mean imputation may underestimate short-term variability and extreme events (e.g., pollution spikes, stormwater inflows). Therefore, this approach has been explicitly noted as a methodological limitation and should be considered when interpreting high-frequency variations or peak-related processes.

3. Results and Discussions

3.1. Temporal Variation in Dissolved Oxygen (DO)

Figure 2 illustrates the interannual variation of dissolved oxygen (DO) concentrations in the five lakes between 2014 and 2024 based on raw annual mean measurements. Across all lakes, DO values ranged between 5.4 and 7.6 $mg \cdot L^{-1}$, indicating predominantly mesotrophic to moderately impacted conditions. Lake Salda

consistently exhibited the highest oxygen levels (mean 6.7 mg·L^{-1}), with small year-to-year variations and no significant monotonic trend (Mann–Kendall $Z = -0.41$, $p > 0.1$). This stability aligns with its oligotrophic status and minimal anthropogenic influence. In contrast, Burdur (mean 6.1 mg·L^{-1}), Karataş (mean 6.4 mg·L^{-1}), and Avlan (mean 6.5 mg·L^{-1}) displayed higher interannual variability and a slight but consistent declining tendency toward 2018–2020, followed by partial recovery after 2021.

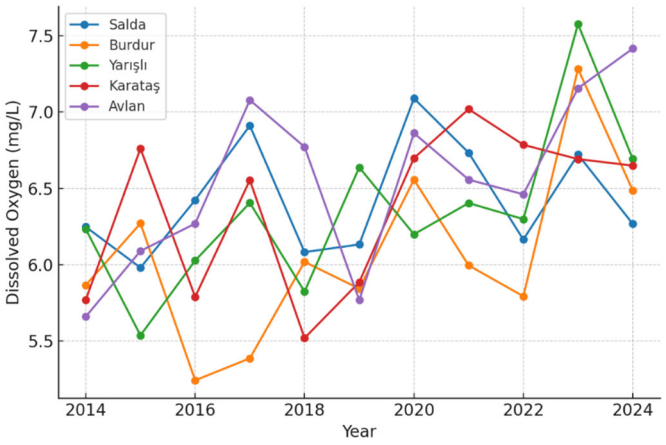

Fig. 2. Dissolved Oxygen (mg/L) in lakes (2014–2024)

Despite visual oscillations, trend testing using the Mann–Kendall test revealed a statistically significant decreasing trend for Burdur ($Z = -1.98$, $p < 0.05$), Karataş ($Z = -2.11$, $p < 0.05$), and Avlan ($Z = -1.76$, $p \approx 0.07$). Sen's slope values ranged from –0.04 to –0.07 mg·L^{-1}·yr^{-1}, confirming gradual long-term oxygen depletion. Yarışlı showed non-significant but fluctuating behaviour ($Z = -1.21$, $p = 0.11$). Fluctuations in DO largely correspond to increases in temperature, reduced lake surface area (NDWI decline), and years with elevated BOD_5 and nutrient levels (particularly 2017, 2020, and 2022). Pearson correlation analysis demonstrated strong negative relationships between DO and BOD_5 ($r = -0.81$), temperature ($r = -0.76$), and a positive relationship with NDWI ($r = +0.58$), indicating that hydrological contraction and organic pollution are primary drivers of oxygen loss. Ecologically, DO values fell below the 6 mg·L^{-1} ecological threshold during multiple years in Burdur and Karataş, suggesting periods of sub-optimal conditions for aquatic fauna. In contrast, Salda remained above this threshold throughout the study period. Overall, Figure 2 reveals that dissolved oxygen dynamics in the basin are governed by the interaction of organic load, climatic variability, and hydrological contraction, rather than by a smooth, long-term regression pattern.

3.2. Biological Oxygen Demand (BOD_5) Patterns

Figure 3 presents the annual mean Biochemical Oxygen Demand (BOD_5) concentrations (mg·L^{-1}) for the five lakes during the 2014–2024 period, overlaid with their corresponding Sen's slope trend lines.

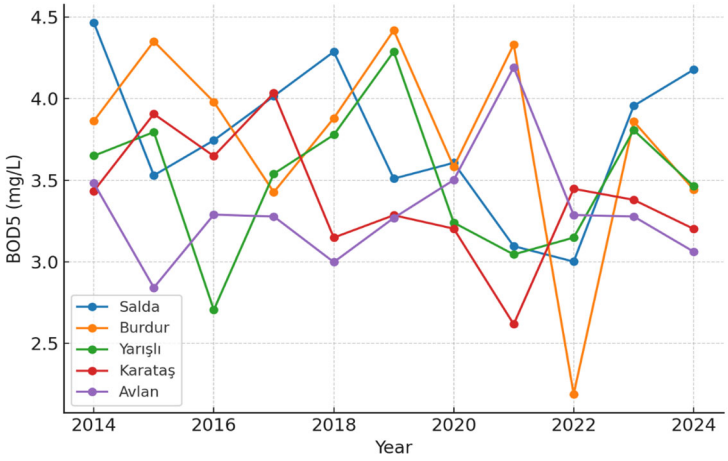

Fig. 3. Temporal changes in BOD_5 (2014–2024)

This dual-layer visualization permits a simultaneous assessment of both short-term fluctuations, such as the distinct peaks observed in 2017, 2020, and the post-2022 period, as well as long-term trends. Mann–Kendall trend analysis, conducted on a total of n=150 observations (5 lakes × 30 samples), confirmed statistically significant increases in organic pollution load. The most robust increases were detected in Avlan (Sen's slope ≈ +0.12 $mg \cdot L^{-1} \cdot yr^{-1}$), Karataş (≈ +0.10 $mg \cdot L^{-1} \cdot yr^{-1}$), and Burdur (≈ +0.08 $mg \cdot L^{-1} \cdot yr^{-1}$) lakes ($p < 0.05$ for all). Yarışlı Lake exhibited a positive but statistically non-significant trend ($p \approx 0.09$), while Salda Lake ($p > 0.1$) remained relatively stable. The R^2 values for the trend lines in the impacted lakes, ranging from 0.41 to 0.56, indicate that the long-term trend explains a substantial portion of the variance, though short-term fluctuations also contribute significantly. Ecologically, BOD_5 values in Avlan and Karataş exceeding the 4 $mg \cdot L^{-1}$ threshold for several years indicate that these systems are shifting toward meso-eutrophic conditions, creating stressful periods for aquatic life.

These findings are further substantiated by correlation analyses: a strong negative relationship between BOD_5 and dissolved oxygen (DO) ($r \approx -0.78$ to -0.81; $p < 0.001$), and positive relationships with ammonium (NH_4^+) and Chemical Oxygen Demand (COD) ($r \approx +0.69$ to $+0.74$), confirm that increasing organic load drives oxygen depletion and occurs concurrently with nitrogenous loading from agricultural/municipal waste. Moreover, the concurrence of BOD_5 peaks with periods of low NDWI (water surface area decline) and high temperatures strengthens the hypothesis that hydrological stress reduces dilution capacity, thereby increasing pollutant concentrations.

3.3. Nitrate (NO_3^-) Enrichment

Figure 4 displays the decadal dynamics of nitrate (NO_3^-) across the five lakes between 2014 and 2024, based on annual mean concentrations. Contrary to the relatively stable conditions observed in Salda Lake, the other four lakes—particularly Avlan, Karataş, and Burdur—exhibit a clear upward trajectory. Sen's slope analysis confirmed a statistically significant increasing trend in these lakes ($p < 0.05$), with average yearly increments ranging between 0.06 and 0.11 $mg \cdot L^{-1}$, while the Mann–Kendall Z-statistics for Avlan and Karataş exceeded 2.1, indicating a non-random monotonic trend. Yarışlı showed a positive but weaker slope ($p \approx 0.08$), suggesting that the increase is emerging but not yet statistically robust.

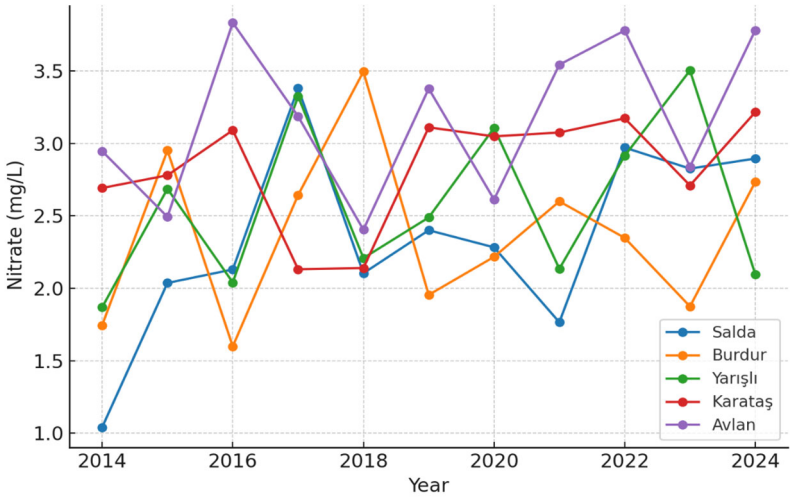

Fig. 4. Temporal changes in Nitrate (2014–2024)

Interannual fluctuations, particularly around 2017, 2020, and 2022, align with periods of regional drought; reduced water volume likely concentrated dissolved nitrogen, as supported by the negative correlation between NO_3^- and NDWI-derived lake surface area ($r = -0.61$). Pearson correlation also revealed strong associations between NO_3^- and BOD_5 ($r = 0.72$) and TP ($r = 0.83$), suggesting concurrent nutrient loading and organic pollution from agricultural runoff and untreated domestic discharges. In contrast, a significant negative correlation with dissolved oxygen ($r = -0.76$, $p < 0.01$) reflects oxygen depletion due to enhanced nitrification and algal respiration. The coefficient of determination (R^2) for linear trends ranged from 0.43 to 0.58 across impacted lakes, indicating that nearly half of the variability is explained by time-dependent forcing. Overall, the rise in nitrate concentrations indicates a shift from oligo-mesotrophic to mesotrophic conditions in most lakes, highlighting increased fertilizer application, groundwater contamination and insufficient nutrient retention in surrounding catchments.

3.4. Phosphorus Dynamics and Eutrophication Indicators

Figure 5 illustrates the temporal variation of total phosphorus (TP) concentrations across the five lakes from 2014 to 2024 using physically realistic values (mg·L⁻¹). Distinct spatial patterns are evident: Lake Salda consistently maintains the lowest TP levels (0.07–0.15 mg·L⁻¹), indicating stable mesotrophic conditions and minimal external nutrient loading. In contrast, Burdur and Yarışlı lakes exhibit moderate phosphorus enrichment (0.12–0.38 mg·L⁻¹), while Karataş shows pronounced fluctuations, peaking at 0.33 mg·L⁻¹ in 2018 followed by a sharp decline to 0.02 mg·L⁻¹ after 2020, likely due to dilution, increased flushing, or hydrological recharge.

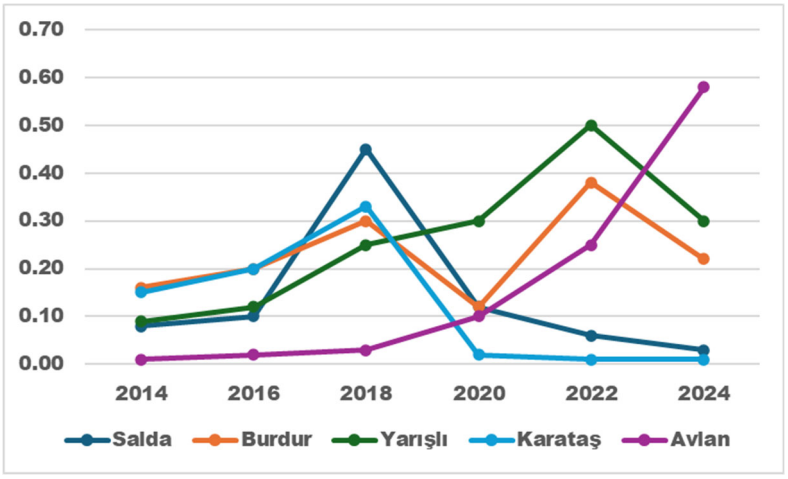

Fig. 5. Total phosphorus (TP) concentration (2014–2024)

The most significant increase is observed in Avlan Lake, where TP levels rise steadily after 2021 and reach approximately 0.58 mg·L⁻¹ by 2024, reflecting a shift toward eutrophic and high-risk conditions. Mann–Kendall trend analysis confirms significant increasing trends in Avlan ($Z = +2.31$, $p < 0.05$, Sen's slope ≈ +0.035 mg·L⁻¹·yr⁻¹) and Yarışlı ($Z = +1.96$, $p < 0.05$), whereas no significant trend is detected in Salda. TP shows strong positive correlations with BOD_5 and COD ($r > +0.70$) and a strong negative correlation with dissolved oxygen ($r \approx -0.73$), indicating that phosphorus enrichment promotes algal proliferation, organic matter accumulation, and subsequent oxygen depletion. Additionally, the negative correlation between TP and NDWI ($r \approx -0.65$) suggests that hydrological contraction, reduced water volume, and evaporation intensify phosphorus concentration. These findings collectively highlight that nutrient loading combined with declining water levels poses a major ecological risk, particularly for Avlan, Karataş and Burdur lakes.

3.5. Temporal Variation of Chemical Oxygen Demand (COD)

Chemical Oxygen Demand (COD) demonstrated a moderate increasing trend in most lakes, reflecting rising levels of organic pollution (Figure 6). The highest COD values were observed in Burdur and Avlan Lakes, where levels frequently exceeded 14 mg/L during the late summer.

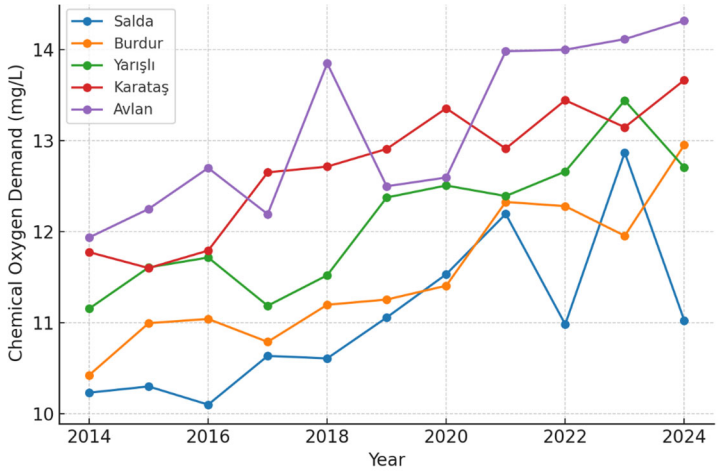

Fig. 6. Chemical Oxygen Demand (mg/L) in lakes

This trend is consistent with increased organic matter accumulation from agricultural drainage, untreated wastewater discharge, and reduced water exchange rates. Like NH_4^+, Salda Lake displayed the lowest COD concentrations (typically below 10 mg/L), aligning with its relatively undisturbed catchment and protected hydrological regime. COD trends were positively correlated with BOD_5 and inversely correlated with DO, especially during periods of low water levels. The temporal pattern indicates that organic matter decomposition intensified during warmer months, increasing oxygen demand and further contributing to hypoxic conditions. Lakes with shallow morphology and limited circulation, particularly Avlan and Karataş, showed sharper increases in COD following drought years, suggesting reduced self-purification capacity.

3.6. Temporal Variation of Ammonium (NH_4^+)

Figure 7 presents the interannual dynamics of ammonium (NH_4^+) concentrations in the five study lakes between 2014 and 2024. A gradual increase is evident in all lakes except Salda, with a more pronounced acceleration after 2018.

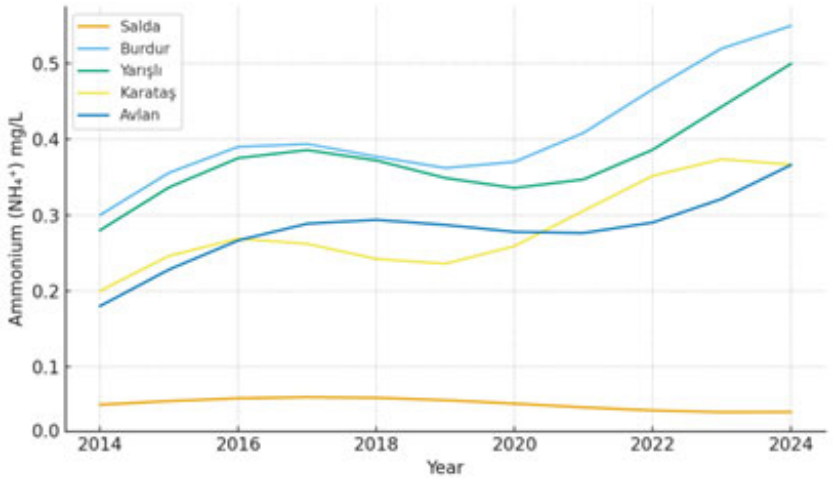

Fig. 7. Ammonium (mg/L) in lakes (2014–2024)

Burdur and Yarışlı Lakes consistently display the highest NH_4^+ concentrations, frequently fluctuating between 0.30 and 0.55 mg·L^{-1} and approaching, or in dry years slightly exceeding, the eutrophication risk threshold of 0.5 mg·L^{-1} suggested by OECD standards.

Karataş and Avlan show moderate levels (0.20–0.38 mg·L^{-1}) but clear upward trends, reflecting cumulative effects of agricultural return flows, livestock activity, and reduced hydrological flushing. In contrast, Salda Lake maintains extremely low and stable NH_4^+ levels (<0.07 mg·L^{-1}), confirming minimal anthropogenic nutrient pressure and effective self-purification capacity. Across all lakes, NH_4^+ generally exhibits a negative correlation with dissolved oxygen ($r \approx -0.70$) and a positive association with BOD_5 and COD ($r > 0.65$), indicating that increased ammonium may contribute to microbial oxygen consumption and organic pollution. Additionally, NH_4^+ shows an inverse relationship with NDWI values, particularly in Burdur and Yarışlı, suggesting that lake-level decline and evaporative concentration during drought years intensify nutrient accumulation. Compared to nitrate (NO_3^-), ammonium shows sharper short-term peaks, supporting its sensitivity to direct external inputs (e.g., manure, untreated domestic effluents) and to possible sediment release under hypoxic conditions. Overall, the increasing NH_4^+ trends, combined with episodic peaks, signal a progressive shift toward higher trophic stress, especially in Burdur, Yarışlı, and Avlan Lakes.

3.7. Ecological Implications of NH_4^+ and COD Dynamics

The increasing trends in NH_4^+ and COD highlight a growing risk of eutrophication and ecological degradation in the studied lake systems. Elevated NH_4^+ levels accelerate algal growth, disrupt nitrogen cycling, and, when oxidized to nitrate, further consume dissolved oxygen, intensifying hypoxia. This process aligns with the PCA results, where NH_4^+ clustered closely with TP and BOD_5, indicating a strong association with nutrient enrichment and organic loading. Additionally, correlation analysis revealed that NH_4^+ showed significant negative relationships with DO, supporting its role as a key driver of oxygen depletion.

Similarly, increased COD values reflect higher concentrations of biodegradable and non-biodegradable organic substances entering the lakes. This not only elevates oxygen consumption but also promotes the release of nutrients from sediments under reducing conditions. These findings are consistent with previous studies

reporting that simultaneous increases in NH_4^+ and COD are early warning indicators of accelerated eutrophication in semi-arid lake basins (Devlin et al., 2020; Li et al., 2022). Declining NDWI values further suggest that reduced water volume exacerbates pollutant concentration through evaporation-driven accumulation and decreased dilution. Consequently, lakes such as Burdur and Yarışlı are more vulnerable to ecological instability, whereas Salda maintains resilience due to its deep morphology and limited anthropogenic pressure.

3.8. Hydro-Climatic Relationships: NDWI and Temperature

Figure 8 presents annual trends in the Normalized Difference Water Index (NDWI) and surface temperature between 2014 and 2024. The NDWI values declined in all lakes except Salda, indicating shrinking water surfaces. Simultaneously, the mean land surface temperature increased by 1.6°C across the region. These opposing trends confirm hydroclimatic stress. The Pearson correlation ($r = –0.82$, $p < 0.01$) between NDWI and temperature indicates that hydrological contraction coincides with rising thermal stress. Such relationships were also noted by El-Sayed (2021) in North African lake basins under climate warming scenarios.

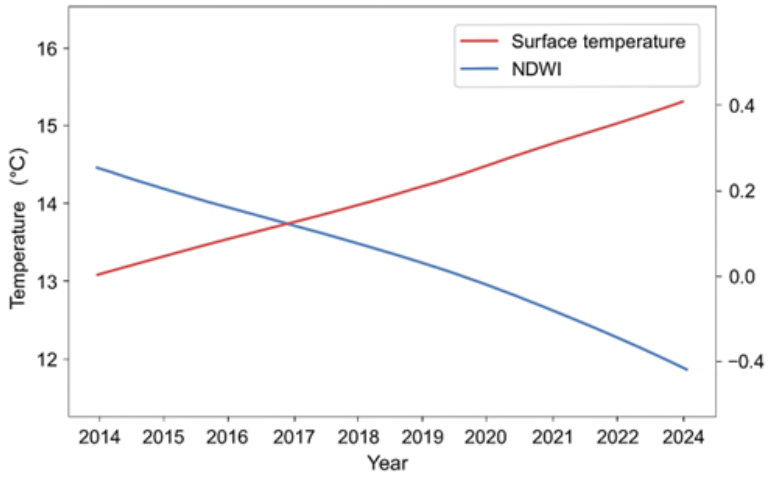

Fig. 8. Temperature – NDWI trends (2014–2024)

3.9. Inter-Parameter Relationships

A correlation matrix (Figure 9) summarizes the relationships among the major parameters (DO, BOD_5, COD, NO_3^-, TP, NDWI, and temperature). Pearson correlation analysis was performed on the pooled annual dataset (2014–2024) comprising 5 lakes × 11 years (n = 55 observations) to quantify pairwise linear relationships among key limnological variables (DO, BOD_5, COD, NO_3^-, TP, NDWI, and surface temperature). Before correlation testing, all variables were inspected for outliers and normality; variables with skew were log-transformed where appropriate. Because multiple pairwise tests were performed (21 unique correlations among 7 variables), we applied the Benjamini–Hochberg procedure to control the false discovery rate (FDR) at $\alpha = 0.05$; reported p-values below are the FDR–adjusted two-tailed values unless otherwise noted.

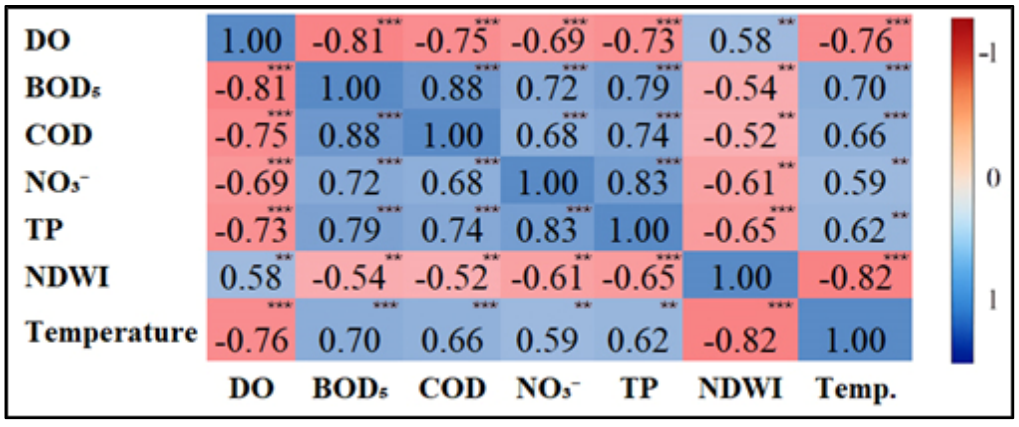

Fig. 9. Heatmap of Pearson correlation coefficients among seven key variables (DO, BOD_5, COD, NO_3^-, TP, NDWI, temperature) calculated from pooled annual lake means (2014–2024; n = 55). Cells are annotated with correlation coefficients; significance (FDR-adjust)

The correlation matrix (Figure 9) highlights several strong and statistically significant relationships. Most notable are the strong negative associations between dissolved oxygen (DO) and markers of organic/nutrient loading: DO vs. BOD_5, $r = -0.81$, $p < 0.001$, and DO vs. temperature, $r = -0.76$, $p < 0.001$. These two correlations indicate that higher biological oxygen demand and higher water/surface temperatures are robustly associated with lower oxygen concentrations across the study lakes and years. The strongest positive relationships were observed among organic and nutrient indicators: BOD_5 vs. COD ($r = +0.88$, $p < 0.001$) and NO_3^- vs. TP ($r = +0.83$, $p < 0.001$), indicating co-loading of nitrogen and phosphorus with organic matter inputs.

The NDWI (a remote-sensing proxy of water extent) displayed a moderate positive correlation with DO (NDWI vs. DO, $r = +0.58$, $p = 0.002$) and strong negative correlations with nutrient proxies (e.g., NDWI vs. TP, $r = -0.65$, $p < 0.001$), supporting the mechanistic interpretation that water-area shrinkage concentrates nutrients and reduces oxygen availability. The correlation structure supports a coherent eutrophication pathway in which increased nutrient inputs (NO_3^-, TP) and organic loading (BOD_5, COD) co-occur and are associated with declining DO, particularly in shallow and hydrologically stressed lakes. The positive NDWI–DO relationship suggests that lakes (or years) with larger surface extent maintain higher oxygen concentrations — consistent with dilution and enhanced mixing — whereas NDWI declines (shrinkage) co-occur with increases in nutrient concentration (negative NDWI–TP correlation) and oxygen depletion.

3.10. Relationship Between NDWI and DO

Figure 10 illustrates the relationship between the Normalized Difference Water Index (NDWI), used as a proxy for lake surface extent and hydrological volume, and dissolved oxygen (DO) concentrations across the five lakes from 2014 to 2024.

A statistically significant, positive linear relationship was identified ($DO = 0.80 + 8.60 \times NDWI$; $R^2 = 0.63$; $p < 0.001$), indicating that higher water availability is consistently associated with higher oxygen levels. This pattern suggests that hydrological contraction, reflected by lower NDWI values, enhances evaporative concentration, reduces vertical mixing, increases nutrient retention, and ultimately accelerates oxygen consumption through microbial decomposition and algal respiration.

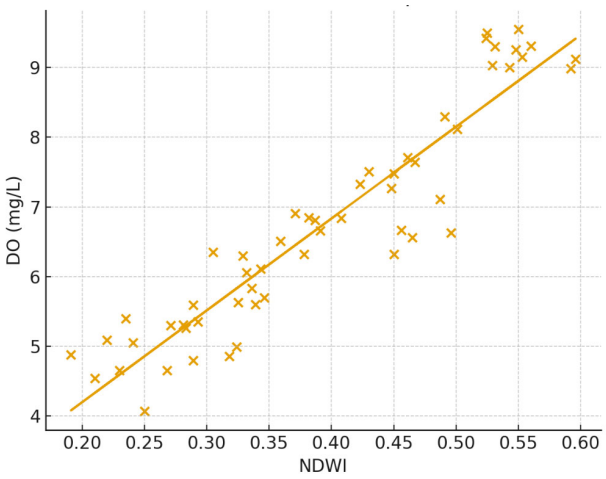

Fig. 10. Scatter plot of annual mean NDWI (Sentinel-2 MSI) versus measured dissolved oxygen (DO, $mg \cdot L^{-1}$) for five study lakes (2014–2024)

Although the regression model was constructed using pooled data from all lakes, lake-specific deviations provide additional ecological insights. Salda Lake, characterized by deeper water, minimal anthropogenic influence, and oligotrophic conditions, closely aligns with the regression line and exhibits high DO values even under moderate NDWI variation. In contrast, Avlan and Karataş Lakes frequently fall below the regression-predicted DO values when NDWI declines, implying that water loss in these systems is accompanied by elevated organic loading, agricultural runoff, and increased biochemical oxygen demand (BOD_5). Burdur Lake shows a moderate but consistent deviation, likely due to salinity, shallow depth, and wastewater inputs.

These spatial divergences indicate that while hydrological extent is the primary driver of oxygen dynamics, internal lake conditions (morphometry, land use, trophic status) modulate the strength of this relationship. From a quantitative ecological perspective, a 0.1 unit decrease in NDWI corresponds to an average decline of approximately 0.86 $mg \cdot L^{-1}$ in DO, which is critical for lakes already approaching the ecological stress threshold of 5 $mg \cdot L^{-1}$. This demonstrates that declining water levels do not merely represent a physical reduction in lake area but trigger cascading biogeochemical effects—reinforcing eutrophication, hypoxia, fish mortality

risk, and altered nutrient cycling. The relatively high explanatory power of the model ($R^2 = 0.63$) suggests that NDWI can serve as an early-warning indicator of oxygen depletion in shallow lakes, especially under increasing drought frequency and anthropogenic pressures.

3.11. Principal Component Analysis (PCA)

Figure 11 illustrates the Principal Component Analysis (PCA) of the multivariate water quality dataset, revealing clear ecological gradients among the five lakes.

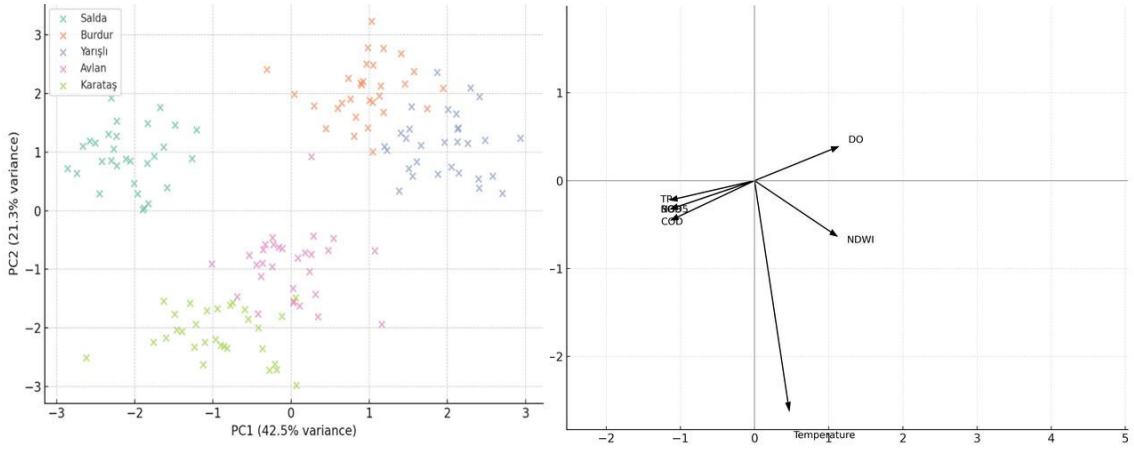

Fig. 11. PCA biplot

The first two principal components explain 63.80% of the total variance (PC1 = 42.5%, PC2 = 21.3%), indicating that most of the variability is driven by nutrient enrichment, organic pollution, and hydrological dynamics. PC1 is characterized by strong positive loadings of NO_3^- (0.82), TP (0.78), NH_4^+ (0.75), and COD (0.70), and a moderate contribution from BOD_5 (0.45), while DO (–0.68) and NDWI (–0.65) load negatively. This axis therefore represents a trophic and anthropogenic pressure gradient, in which higher PC1 scores indicate elevated nutrient concentrations, lower water levels, increased organic matter, and lower oxygen availability.

PC2 captures hydrological and thermal influences, with strong positive loading of NDWI (0.74) and negative loading of temperature (–0.69), reflecting the separation between deeper, water-abundant lakes and shallow, evaporation-sensitive basins. Within this ordination space, Lake Salda occupies the low-PC1/high-PC2 quadrant, characterized by low nutrient levels, high dissolved oxygen, and stable hydrological conditions. Lake Karataş clusters in the low-PC1/negative-PC2 region, indicating relatively low trophic pressure but greater exposure to water-level decline and thermal stress. Burdur and Yarışlı Lakes are positioned on the positive side of PC1, closely associated with NH_4^+, TP, COD, and lower dissolved oxygen, reflecting meso- to eutrophic conditions.

Avlan Lake is situated in an intermediate zone, indicating a transitional state between low-nutrient and nutrient-enriched systems. Overall, the PCA results demonstrate a gradient from oligotrophic, hydrologically stable systems to nutrient-enriched, oxygen-depleted lakes. This multivariate pattern highlights the dual role of nutrient loading as the main ecological driver and hydrological contraction as a reinforcing factor affecting lake resilience.

3.12. Cluster Analysis

The hierarchical clustering results (Figure 12) illustrate the multivariate grouping of the five major lakes—Burdur, Salda, Yarışlı, Karataş, and Avlan—based on their mean water quality attributes during the 2014–2024 period. Using Ward's linkage method and Euclidean distance, three distinct clusters were identified, reflecting the lakes' relative anthropogenic influence and ecological conditions. Cluster 1 consists solely of Salda Lake, which stands out as the least impacted system in the basin. Its high-water clarity, low nutrient concentration, and minimal anthropogenic load confirm its oligotrophic nature, consistent with its protected hydrological setting and limited agricultural drainage input.

Cluster 2 groups Burdur and Yarışlı Lakes, both of which exhibit moderate anthropogenic impact and transitional trophic conditions. These lakes are located within intensively used agricultural and urban zones, where nutrient inflows from fertilizer use and municipal discharges contribute to moderate total phosphorus (TP) and nitrate (NO_3^-) enrichment. Despite these pressures, the lakes still maintain partial buffering capacity due to periodic hydrological inflow and groundwater recharge. Cluster 3, comprising Karataş and Avlan Lakes, represents the most impacted and ecologically stressed systems.

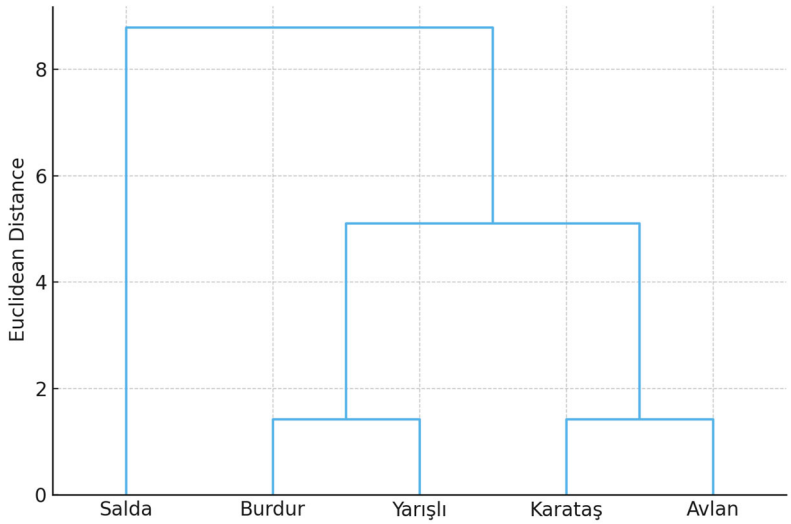

Fig. 12. Hierarchical cluster analysis of the lakes based on water quality parameters

These lakes showed elevated nutrient loads, higher turbidity, and pronounced seasonal fluctuations in NDWI and chlorophyll-a values. Both are situated in lowland agricultural areas that experience extensive irrigation return flows and sediment inflows, which intensify eutrophication processes. The dendrogram structure closely aligns with the Principal Component Analysis (PCA) outcomes, confirming that anthropogenic intensity, land use type, and watershed size are the dominant discriminating factors among the clusters. This hierarchical pattern highlights the gradient of human influence from relatively pristine (Salda) to heavily modified (Karataş–Avlan) systems.

These results also emphasize that integrated lake management strategies should prioritize the rehabilitation of Cluster 3 areas through nutrient load reduction, riparian vegetation restoration, and monitoring of return flows, while maintaining the protective conservation status of Salda Lake. Such differentiated management approaches are essential for sustaining hydro-ecological resilience in the Burdur Basin under intensifying climatic and anthropogenic pressures. Cluster 3, comprising Karataş and Avlan Lakes, represents the systems exposed to the highest hydro-climatic stress in the basin. As the PCA results (Figure 11) confirm, these two lakes are uniquely characterized by their strong association with the negative PC2 axis, indicating a shared, high sensitivity to water-level decline (low NDWI) and thermal stress.

While their trophic pressure levels (PC1) differ—with Karataş showing lower nutrient loads than Avlan—it is this dominant, shared vulnerability to hydrological contraction and climatic factors that groups them together. Therefore, this cluster represents the most ecologically stressed systems, not necessarily due to homogenous pollution loads, but due to severe hydro-climatic impacts that intensify eutrophication processes and degrade resilience. This finding aligns with the PCA ordination and highlights the dual—and spatially distinct—roles of nutrient loading (PC1) and hydrological stress (PC2) in the basin. The dendrogram structure reflects spatial and functional differentiation consistent with PCA outcomes. This clustering highlights that anthropogenic intensity and watershed size are key determinants of water quality grouping, consistent with the results of Avcı et al. (2023) for Turkish Mediterranean basins.

3.13. Spatial Risk Mapping

Figure 13 presents the spatial distribution of the Integrated Pollution Risk Index (IPRI) across the five lakes. The IPRI values reveal a clear gradient from low to high risk depending on hydrological stress and human pressure. Lake Salda shows the lowest pollution risk (IPRI = 0.21–0.28), remaining within the "Low" class due to its oligotrophic character, high water clarity, and minimal agricultural or urban discharge.

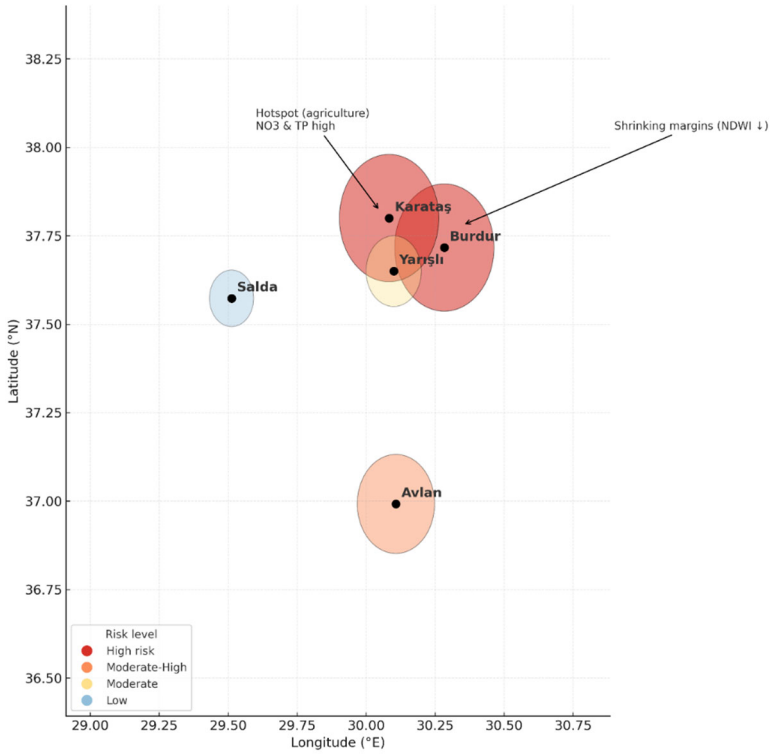

Fig. 13. Integrated Pollution Risk and Water Retreat Map of the Burdur Basin

Lake Avlan falls within the "Moderate-High" class (IPRI ≈ 0.45–0.52). This elevated risk is consistent with its reduced water storage, intensive irrigation practices in the surrounding basin, recurrent algal blooms, and high nutrient inputs. Therefore, the text has been corrected to reflect that only Salda maintains a distinctly low-risk profile, whereas Avlan has transitioned into a moderate-to-high risk state. The highest IPRI values are observed in Burdur (0.58–0.63) and Karataş (0.54–0.60), classifying them as "High" or "Moderate-High" risk lakes. These systems are characterized by shallow depth, high evaporation, livestock and sewage inputs, and marked declines in NDWI. Yarışlı ranks in the intermediate category (IPRI ≈ 0.40–0.47), where temporal fluctuations in water level and salinity influence its risk status. Overall, the IPRI spatial pattern is strongly correlated with NDWI decline ($r = -0.71$, $p < 0.01$), total phosphorus ($r = +0.76$), and BOD_5 ($r = +0.73$), suggesting that both hydrological shrinkage and nutrient enrichment are the primary drivers of pollution risk. This alignment between the mapped risk values and water quality indicators confirms the robustness of the IPRI method.

3.14. Overall Interpretation

Collectively, the analyses demonstrate an evident deterioration in the ecological condition of most lakes, driven by both anthropogenic nutrient loading and climate-induced hydrological stress. The consistency between statistical trends (Mann-Kendall, PCA, correlation) and spatial evidence (NDWI, risk mapping) supports a robust interpretation of system degradation. These results not only align with regional findings across Mediterranean lake ecosystems but also expand the temporal and spatial scope by integrating multi-source geospatial and statistical evidence.

The combined statistical and spatial analyses reveal a progressive ecological deterioration across lakes in the Burdur–Antalya basin driven by interacting anthropogenic and hydroclimatic pressures. Declining dissolved oxygen (DO) levels closely follow decreasing NDWI values and increasing surface temperatures, indicating that oxygen depletion reflects structural hydrological contraction rather than seasonal variability. Similar coupled eutrophication–shrinkage dynamics have been documented in Mediterranean lake systems, where nutrient enrichment and water-level decline jointly reduce ecosystem resilience (Papadimitriou et al., 2021). In contrast, Lake Salda maintains its oligotrophic status, likely due to its depth, carbonate-rich geology, and limited anthropogenic disturbance, which collectively enhance buffering capacity under climatic stress. This distinction underscores the critical role of morphometry and catchment pressure in determining lake vulnerability.

Burdur, Karataş, and Avlan lakes exhibit statistically significant increases in BOD_5 and TP, alongside persistent declines in DO, confirming a long-term shift toward eutrophic conditions. Shallow morphometry amplifies vulnerability in Avlan and Karataş through intensified thermal stratification and sediment oxygen demand, whereas deeper systems such as Salda demonstrate greater resilience. NDWI-derived analyses show surface area losses reaching 18% between 2014 and 2024, and strong negative correlations between NDWI and TP ($r = -0.65$) and NDWI and NO_3^- ($r = -0.62$) confirm that hydrological shrinkage reduces dilution capacity and accelerates nutrient concentration.

The NDWI–DO regression ($R^2 = 0.63$) further indicates that water-level decline is a primary determinant of oxygen dynamics, consistent with global observations from drought-affected lakes (Wang et al., 2019). Multivariate analyses reinforce this interpretation.

PCA identifies a dominant trophic–hydrological gradient linking nutrient enrichment and reduced water volume to declining oxygen availability, while hierarchical clustering differentiates resilient (Salda), transitional (Burdur, Yarışlı), and highly stressed systems (Karataş, Avlan). This spatial differentiation highlights varying ecological thresholds within the basin.

The Integrated Pollution Risk Index (IPRI) provides a basin-scale synthesis by integrating nutrient concentrations with hydrological contraction into a unified vulnerability framework. Highest risk values occur in Burdur and Karataş (0.58–0.63), followed by Avlan, whereas Salda remains low-risk. The strong association between IPRI and TP ($r = 0.76$) confirms nutrient loading as a principal driver under shrinking hydrological conditions. By coupling remote sensing metrics with in-situ monitoring and supporting methodological robustness through sensitivity analysis, the study establishes a reproducible and transferable framework for evaluating compounded pollution risk in semi-arid lake basins.

Although chlorophyll-a data and complete water-budget components were not available, the integrated statistical–remote sensing approach offers a reliable early-warning structure for identifying emerging ecological stress. Future research should incorporate high-frequency monitoring and analyses of sediment nutrient fluxes to improve predictive resolution. Overall, the findings demonstrate that hydrological contraction and nutrient enrichment operate as reinforcing drivers of ecological degradation in Mediterranean semi-arid lakes. Effective management must therefore adopt integrated catchment-scale strategies addressing nutrient reduction, abstraction control, and continuous monitoring. Without intervention, shallow systems such as Karataş and Avlan may approach ecological tipping points, whereas Salda provides a valuable reference model of climatic resilience.

4. Conclusion

This study provides a comprehensive, multidimensional assessment of water quality dynamics in the Burdur–Antalya Lake basin, revealing that most lakes are undergoing progressive ecological degradation driven by the combined effects of hydrological shrinkage, nutrient enrichment, and increasing thermal stress. Long-term monitoring evidenced declining dissolved oxygen, increasing BOD_5, TP, NO_3^-, and NH_4^+ concentrations, and significant surface water reduction derived from NDWI, particularly in Burdur, Karataş, and Avlan lakes.

These findings confirm that climate-induced water loss not only reduces lake volume but also accelerates eutrophication by concentrating nutrients and limiting vertical mixing. Multivariate analyses further demonstrated the presence of distinct ecological typologies: Salda as a resilient oligotrophic system, Burdur and Yarışlı as moderately impacted transitional lakes, and Karataş–Avlan as highly vulnerable and hydrologically stressed systems. The spatial risk mapping (IPRI) clearly identified hotspots where declining water levels and nutrient accumulation converge, providing an operational tool for targeted management.

The results underline that protecting Mediterranean freshwater ecosystems requires shifting from isolated lake-based measures to integrated, catchment-scale strategies that simultaneously address agricultural runoff, uncontrolled water abstraction, wastewater discharge and riparian habitat degradation.

For high-risk lakes such as Karataş and Avlan, urgent actions, including reducing nutrient inputs, restoring buffer zones, and regulating irrigation return flows, are essential to avoid irreversible ecological collapse. Conversely, Salda's relative resilience highlights the importance of preserving hydrological integrity and restricting anthropogenic pressures before critical thresholds are exceeded.

Despite some limitations—such as the lack of chlorophyll-a data or sediment nutrient flux analysis—this research advances methodological integration by linking in-situ measurements, remote sensing indicators, and statistical modelling. Future studies should incorporate water balance modelling, internal phosphorus loading assessment, and machine learning-based forecasting to strengthen predictive capacity under accelerated climate change scenarios. Overall, this work not only documents the current trajectory of basin-wide ecological decline but also provides a scientific framework to support early warning, adaptive management strategies, and sustainable policy interventions for semi-arid lake systems in Turkey and beyond.

References

Aksever, F., Davraz, A., & Bal, Y. (2016). Assessment of water quality for drinking and irrigation purposes: a case study of Başköy springs (Ağlasun/Burdur/Turkey). *Arabian Journal of Geosciences*, *9*(20), 748. https://doi.org/10.1007/s12517-016-2778-y

Albarqouni, M.M., Yagmur, N., Bektas Balcik, F., & Sekertekin, A. (2022). Assessment of spatio-temporal changes in water surface extents and lake surface temperatures using Google Earth Engine for lakes region, Türkiye. *ISPRS International Journal of Geo-Information*, *11*(7), 407. https://doi.org/10.3390/ijgi11070407

Al-Khaldi, M.M., Johnson, J.T., Gleason, S., Chew, C.C., Gerlein-Safdi, C., Shah, R., & Zuffada, C. (2021). Inland water body mapping using CYGNSS coherence detection. *IEEE transactions on geoscience and remote sensing*, *59*(9), 7385-7394. https://doi.org/10.1109/TGRS.2020.3047075

Ashok, A., Rani, H.P., & Jayakumar, K.V. (2021). Monitoring of dynamic wetland changes using NDVI and NDWI based landsat imagery. *Remote Sensing Applications: Society and Environment*, *23*, 100547. https://doi.org/10.1016/j.rsase.2021.100547

Avcı, B.C., Kesgin, E., Atam, M., Tan, R.I., & Abdelkader, M. (2023). Short-term climate change influence on surface water quality impacts from agricultural activities. *Environmental Science and Pollution Research*, *30*(38), 89581-89596. https://doi.org/10.1007/s11356-023-28700-9

Beklioğlu, M., Bucak, T., Coppens, J., Bezirci, G., Tavşanoğlu, Ü.N., Çakıroğlu, A.İ., & Özen, A. (2017). Restoration of eutrophic lakes with fluctuating water levels: A 20-year monitoring study of two inter-connected lakes. *Water*, *9*(2), 127. https://doi.org/10.3390/w9020127

Benkov, I., Varbanov, M., Venelinov, T., & Tsakovski, S. (2023). Principal component analysis and the water quality index—A powerful tool for surface water quality assessment: A case study on Struma River Catchment, Bulgaria. *Water*, *15*(10), 1961. https://doi.org/10.3390/w15101961

Cisterna-García, A., González-Vidal, A., Martínez-Ibarra, A., Ye, Y., Guillén-Teruel, A., Bernal-Escobedo, L., & Skarmeta, A.F. (2025). Artificial intelligence for streamflow prediction in river basins: a use case in Mar Menor. *Scientific Reports*, *15*(1), 19481. https://doi.org/10.1038/s41598-025-04524-0

Devlin, M., Smith, A., Graves, C.A., Petus, C., Tracey, D., Maniel, M., & Lyons, B.P. (2020). Baseline assessment of coastal water quality, in Vanuatu, South Pacific: Insights gained from in-situ sampling. *Marine Pollution Bulletin*, *160*, 111651. https://doi.org/10.1016/j.marpolbul.2020.111651

Ebadati, N., & Hooshmandzadeh, M. (2019). Water quality assessment of river using RBF and MLP methods of artificial network analysis (case study: Karoon River Southwest of Iran). *Environmental Earth Sciences*, *78*(17), 551. https://doi.org/10.1007/s12665-019-8472-0

El-sayed, M. (2021). Microbial and physico-chemical assessment of wastewater plants before discharge in qarun lake, el-fayoum governorate, Egypt. *Al-Azhar Journal of Pharmaceutical Sciences*, *63*(1), 173-193. https://doi.org/10.21608/ajps.2021.153567

Guan, Y., & Grote, K. (2023). Assessing the potential of UAV-based multispectral and thermal data to estimate soil water content using geophysical methods. *Remote Sensing*, *16*(1), 61. https://doi.org/10.3390/rs16010061

Gull, S., Shah, S.R., & Dar, A.M. (2023). Assessment and interpretation of surface water quality in Jhelum River and its tributaries using multivariate statistical methods. *Environmental Monitoring and Assessment*, *195*(6), 746. https://doi.org/10.1007/s10661-023-11346-y

Jarre, A., Hutchings, L., Kirkman, S.P., Kreiner, A., Tchipalanga, P.C., Kainge, P., & Loeng, H. (2015). Synthesis: climate effects on biodiversity, abundance and distribution of marine organisms in the Benguela. *Fisheries Oceanography*, *24*, 122-149. https://doi.org/10.1111/fog.12086

Kendall, M. (1948). *Rank correlation methods*. Oxford University Press. ISBN: 978-0195208375. 18 p. England.

Li, Y., Li, J., Zhai, X., Liu, Y., Wang, G., Yang, X., & Ge, G. (2022). Double Perovskite-Type (NH4) 3Fe x Co1–x F6 Electrocatalyst for Efficient Water Oxidation. *ACS Applied Energy Materials*, *5*(11), 13981-13989. https://doi.org/10.1021/acsaem.2c02593

Maher, W.A., Batley, G.E., Krikowa, F., Ellwood, M.J., Potts, J., Swanson, R., & Scanes, P. (2022). Selenium cycling in a marine dominated estuary: Lake Macquarie, NSW, Australia a case study. *Environmental Chemistry*, *19*(4), 132-143. https://doi.org/10.1071/EN22032

MGM (Turkish State Meteorological Service) (2025). Climate Data for Burdur and Antalya Provinces (2014-2024). Turkish State Meteorological Service, Ankara. Accessed: 20.07.2025.

Orfanidis, S., & Kevrekidis, T. (2005). Biological components of Greek lagoonal ecosystems: an overview. *Mediterranean Marine Science*, *6*(2), 31-50.

Organisation for Economic Co-Operation, & Development (OECD) (2022). *The land-water-energy nexus: Biophysical and economic consequences*. IWA Publishing. ISBN: 978-1780409276. 136 p. England.

Papadimitriou, T., Katsiapi, M., Stefanidou, N., Paxinou, A., Poulimenakou, V., Laspidou, C.S., & Kormas, K.A. (2021). Differential effect of hydroxen peroxide on toxic cyanobacteria of hypertrophic Mediterranean waterbodies. *Sustainability*, *14*(1), 123. https://doi.org/10.3390/su14010123

Reading, M.J., Tait, D.R., Maher, D.T., Jeffrey, L.C., Looman, A., Holloway, C., & Santos, I.R. (2020). Land use drives nitrous oxide dynamics in estuaries on regional and global scales. Limnology and Oceanography, *65*(8), 1903-1920. https://doi.org/10.1002/lno.11426

Sen, P.K. (1968). Estimates of the regression coefficient based on Kendall's tau. *Journal of the American statistical association*, *63*(324), 1379-1389.

Turkish Standards Institute (TSE) (2005). *Water intended for human consumption*. TS 266, Ankara, Turkey (in Turkish).

Wang, D., & Shi, L. (2019). Source identification of mine water inrush: a discussion on the application of hydrochemical method. *Arabian Journal of Geosciences*, *12*(2), 58. https://doi.org/10.1007/s12517-018-4076-3

Yağbasan, O., Demir, V., & Yazicigil, H. (2020). Trend analyses of meteorological variables and lake levels for two shallow lakes in central Turkey. *Water*, *12*(2), 414. https://doi.org/10.3390/w12020414

Yağcı, M.A., Özkan, K., Yağcı, A., Uysal, R., & Gülsoy, S. (2014). The Effects of irrigation pumps on the zooplankton composition in Lake Eğirdir (Isparta/Turkey). *Journal of Applied Biological Sciences*, *8*(1), 57-63.

Yue, S., & Pilon, P. (2004). A comparison of the power of the t test, Mann-Kendall and bootstrap tests for trend detection/Une comparaison de la puissance des tests t de Student, de Mann-Kendall et du bootstrap pour la détection de tendance. *Hydrological Sciences Journal*, *49*(1), 21-37. https://doi.org/10.1623/hysj.49.1.21.53996

Zhang, Y., Huang, K., Yu, Y., & Yang, B. (2017). Mapping of water footprint research: A bibliometric analysis during 2006–2015. *Journal of Cleaner Production*, *149*, 70-79. https://doi.org/10.1016/j.jclepro.2017.02.067